ADVANCED FUNCTIONAL MATERIALS

FULL PAPER

DOI: 10.1002/adfm.200700231

Tuning the Emitting Color of Organic Light-Emitting Diodes Through Photochemically Induced Transformations: Towards Single-Layer, Patterned, Full-Color Displays and White-Lighting Applications

By *Maria Vasilopoulou*,* *Dimitra Georgiadou*, *George Pistolis*, and *Panagiotis Argitis**

Photochemically induced emission tuning for the definition of pixels emitting the three primary colors, red, green, blue (RGB), in a single conducting polymeric layer is investigated. The approach proposed is based on an acid-induced emission shift of the (1-[4-(dimethylamino)phenyl]-6-phenylhexatriene) (DMA-DPH) green emitter and acid-induced quenching of the red fluorescent emitter (4-dimethylamino-4′-nitrostilbene) (DANS). The two emitters are dispersed in the wide bandgap conducting polymer poly(9-vinylcarbazole) (PVK), along with a photoacid generator (PAG). In the unexposed film areas, red emission is observed because of efficient energy transfer from PVK and DMA-DPH to DANS. Exposure of selected areas of the film at different doses results in quenching of the red emitter's fluorescence and the formation of green, blue, or even other color-emitting pixels, depending on the exposure dose and the relative concentrations of the different compounds in the film. Organic light-emitting diodes having the PVK polymer containing the appropriate amounts of DMA-DPH, DANS, and PAG as the emitting layer are fabricated and electroluminescence spectra are recorded. The time stability of induced emission spectrum changes and the color stability during device operation are also examined, and the first encouraging results are obtained.

1. Introduction

Organic light-emitting diodes (OLEDs), since their invention, have been the subject of intense scientific and technological investigation.[1–3] A lot of progress has already been achieved but further technological developments are needed for their successful implementation in application areas such as displays and lighting. For instance, the generation of a full-color image in a display requires the existence of nearby discrete areas, which are capable of emitting one of the three primary colors, red, green, or blue (RGB), and several techniques have appeared in order to produce the three-color-emitting pixels. In general, the manufacture of a full-color display involves the formation of multilayer OLED structures[4] and requires deposition and patterning of usually different organic layers one over the other, where each one is capable of emitting one of the three main colors. Another common technique for the fabrication of full-color devices is ink-jet printing,[5] which has the advantages of low cost and little material loss. However, there are also issues to be solved in this case such as limitations in the achievable resolution and thickness homogeneity.

Similar challenges are encountered in white-light-emitting diodes, which have potential for use in the next generation of sources for solid-state lighting.[6] White-light emission can also be obtained from a single-layer copolymer,[7] from polymer blends,[8] or from devices based on fluorescent[9a] and phosphorescent[9b–d] dye-dispersed hosts (polymers or small molecules), while recently blue fluorescent along with green and red phosphorescent doped devices have been reported.[10] On the other hand, excimer- and exciplex-based emission from a single layer can appear at various wavelengths, and, thus, it is also possible to achieve white-light emission following this route.[11]

Recently, alternative photopatterning approaches for light-emitting diodes based on conjugated polymers (PLEDs) have been proposed.[12,13] Full-color photopatterned light-emitting devices have been presented by Shirai and Kido,[12a] who used laser irradiation to bleach dye molecules in a poly(*N*-vinylcarbazole) matrix, while other approaches employ selective photobleaching[12b,d] or tuning[12c] of the emission properties of a single layer that consists of polymer blends for RGB emission. In a different approach Müller et al.[13a] and Gather et al.[13b] were able to demonstrate RGB devices by sequential patterning by means of solution processing and photocrosslinking of red-, green-, and blue-emitting polymer layers.

[*] Dr. M. Vasilopoulou, Dr. P. Argitis, D. Georgiadou
Institute of Microelectronics, NCSR "Demokritos"
153 10 Aghia Paraskevi, Attiki (Greece)
E-mail: mariva@imel.demokritos.gr; argitis@imel.demokritos.gr
Dr. G. Pistolis
Institute of Physical Chemistry, NCSR "Demokritos"
153 10 Aghia Paraskevi, Attiki (Greece)

[**] This research has been conducted within the framework of the "Archimedes: Funding of research groups in TEI of Piraeus" project, co-funded by the European Union (75 %) and the Greek Ministry of Education (25 %).

Technological approaches that could improve the current materials and processes used in OLEDs could also be based on recent advances reported in the related field of fluorescence imaging in polymeric thin films. The investigation of fluorescence-patterning possibilities in thin polymeric films has recently emerged as a broader topic of research for the development of plastic materials suitable for, amongst other things, lighting, image recording, sensing, and display applications.[14] It should also be added that fluorescent organic dyes dispersed in the polymer film, or moieties pending to the polymer itself, have been used for fluorescence imaging to monitor acid diffusion in the area of lithographic processing,[15] where acid-induced changes of emission properties usually result in the production of fluorescent and nonfluorescent areas (acid-induced dye quenching).[14,15]

In this work we present a new patterning scheme for functional organic thin films based on energy transfer to suitable emitters, the spectrum of which is altered by photochemical transformations. In particular, changes initiated by photogenerated acids determine the extent of energy transfer and induce emission tuning, enabling the definition of different color-emitting areas in a polymeric layer. Our first effort[16] to use a photoacid-generation approach for bicolor imaging in nonconducting matrixes is further exploited to develop photopatterning schemes for the definition of RGB areas in a wide bandgap conductive polymer matrix. Definition of areas emitting red, green, and blue in a single layer is demonstrated, and possibilities for the application of the proposed imaging strategy to OLED technology are investigated and discussed.

2. Results and Discussion

2.1. Emission Tuning of the Green Emitter in a Conducting Matrix

Previously we reported an extensive spectroscopic study[16] on acid-induced absorbance and emission shifts of the green fluorescenct 1-[4-(dimethylamino)phenyl]-6-phenylhexa-1,3,5,-triene (DMA-DPH). Briefly, it was found that the emission wavelength of DMA-DPH is very sensitive to the micropolarity of its immediate environment.[16b,c] The observed sizable spectral shifts of DMA-DPH arise from charge delocalization in the extended conjugated system of the molecule induced by the electron-donating effect of the *p*-dimethylamino group. It was shown that photoinduced protonation of the dimethylamino group in DMA-DPH can disrupt the conjugation and, as a consequence, could hypsochromically shift the DMA-DPH absorption and emission maxima to lower blue wavelengths. These spectral changes have been demonstrated in films based on poly(methyl methacrylate) (PMMA) and on aromatic rings containing an epoxy novolac polymer.[16a]

In the present investigation, we first examined if similar changes can also be observed in conducting matrices used in OLEDs. Poly(9-vinylcarbazole) (PVK)[17] was used as the host matrix, as its emission peak located is in the violet-blue region (at 413 nm), and, moreover, PVK is well-known for efficient energy transfer to fluorescent[17b] and phosphorescent[17c] organic molecules with lower-energy excited states. Efficient energy transfer to the green emitter DMA-DPH was first demonstrated, as shown in Figure 1a (unexposed). A small concentration of the emitter in the matrix (2 % w/w) can lead to the total elimination of the emission of PVK and to the appearance of the characteristic spectrum of DMA-DPH (maximum at approximately 500 nm). The addition of a selected photoacid generator (PAG) in the matrix, which in this case was the triphenylsulfonium trifluoromethane sulfonate, does not alter the energy-transfer efficiency.

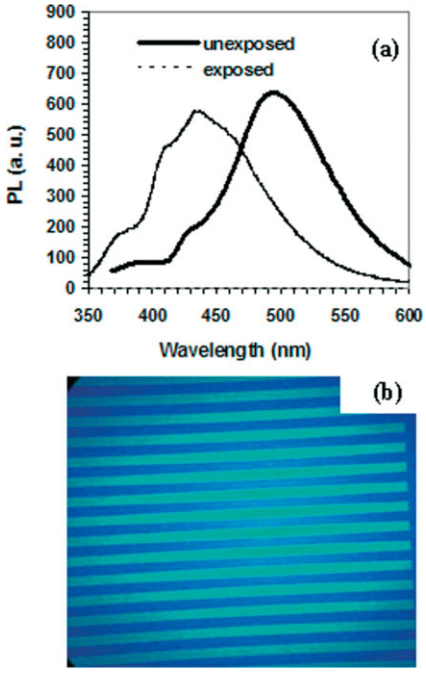

Figure 1. a) Photoluminescence (PL) spectra of a VK film (100 nm thick) containing the DMA-DPH emitter and the photoacid generator (PAG), triphenylsulfonium trifluoromethane sulfonate, at concentrations of 2 % and 4 % of the polymer mass (w/w), respectively, before and after exposure through a 248 nm narrow band filter for 1000 s (the excitation wavelength was 340 nm). b) Fluorescence patterns obtained with the same PVK film as in (a). The blue areas are the regions exposed through the photomask. Line width: 15 μm.

It should be noted that in our first experiments the PAG used was the triphenylsulfonium hexafluoroantimonate [$(Ph_3S^+)(SbF_6^-)$]. In these experiments, we observed that after the addition of this particular PAG, the emission of DMA-DPH inside the PVK matrix was dramatically decreased. A possible explanation of this behavior could be that the heavy atom Sb, present in the PAG anion, causes quenching of the PVK emission. Thus, it was decided to use onium salts with all organic anions, and triphenylsulfonium trifluoromethane sulfonate ($SPh_3^+ CF_3SO_3^-$) was selected because it has the same cation as triphenylsulfonium hexafluoroantimonate. A clear photochemically induced fluorescence shift was obtained by using the triphenylsulfonium trifluoromethane sulfonate as PAG, as

ADVANCED FUNCTIONAL MATERIALS

is shown in Figure 1a ("exposed" curve). After exposure at a wavelength of $\lambda = 248$ nm, where only the PAG absorbs strongly, the photogenerated acid indeed protonates the dimethylamino group of DMA-DPH, as is proven by the 60 nm hypsochromic shift observed in the absorption spectrum of the unexposed film (maximum at 500 nm) compared to that of the exposed film (maximum at 440 nm).

Color patterning is illustrated in Figure 1b. The exposure of PVK films containing the DMA-DPH emitter and the PAG through a photolithographic mask results in the generation of acid in selected film areas and in the definition of blue and green lines in the films. At this point it should be mentioned that the lateral diffusion of the photogenerated acid in the polymer matrix does not appear to be a problem, as DMA-DPH bears strongly basic amine groups and proton capture is very efficient. On the other hand, it should be noted that the resolution requirements in our case are relaxed compared to the demands of standard photoresist technology where imaging at the sub-micrometer level and below is required.

The stability of the DMA-DPH form obtained after photoprotonation was examined in a PMMA matrix, where the monitoring of any changes in the absorption spectrum is straightforward because PMMA is transparent in the region of interest. On the contrary, the absorption spectrum of PVK within this region overlaps with that of DMA-DPH and makes it difficult to observe any absorption spectrum changes. It was first observed that after several hours under ambient conditions the blue-emitting areas returned to green, an indication of deprotonation of the DMA-DPH molecule. Indeed, as can be seen in Figure 2a, the absorption spectrum of the emitter after protonation is not stable and returns to its original position after a certain number of hours in air. This reverse change is attributed to proton consumption by an antagonist in the matrix. It is very well-known[18,19] that even a very small amount—in the ppb range—of basic contaminants, which can be absorbed from the atmosphere, is enough to alter the lithographic results in acid-catalyzed resist systems. In this case, acid consumption can lead to deprotonation of the emitter and the return to its original chemical form.

To deal with this undesirable shift in the spectrum of the emitter to its initial position, the effect of thermal treatment before exposure (prebake at increased temperature) was examined, in order to decrease the free volume in the film and thus to reduce the diffusion of basic contaminants from the atmosphere inside the polymeric film. It has actually been reported before that prebake at high temperature (above the glass-transition temperature) greatly increases environmental stability in chemically amplified photoresists, and the development of a photoresist class called ESCAP (environmentally stable chemically amplified positive resists) is based on this finding.[18] In our case it was indeed found that optimization of the conditions for film preparation (by increasing the prebake temperature) and storage could help overcome the problem of undesirable spectral changes, as shown in Figure 2b and c. Here, the absorption spectra of PMMA films containing the DMA-DPH emitter and the PAG, which were prebaked at a higher temperature (130 °C instead of 70 °C) (Fig. 2b) or stored under reduced pressure (Fig. 2c), appear stable even after one week. Alternatively, the use of an overcoat to hinder diffusion of basic environmental contaminants also led to stability improvement in accordance with results reported by others in chemically amplified photoresist technology.[19]

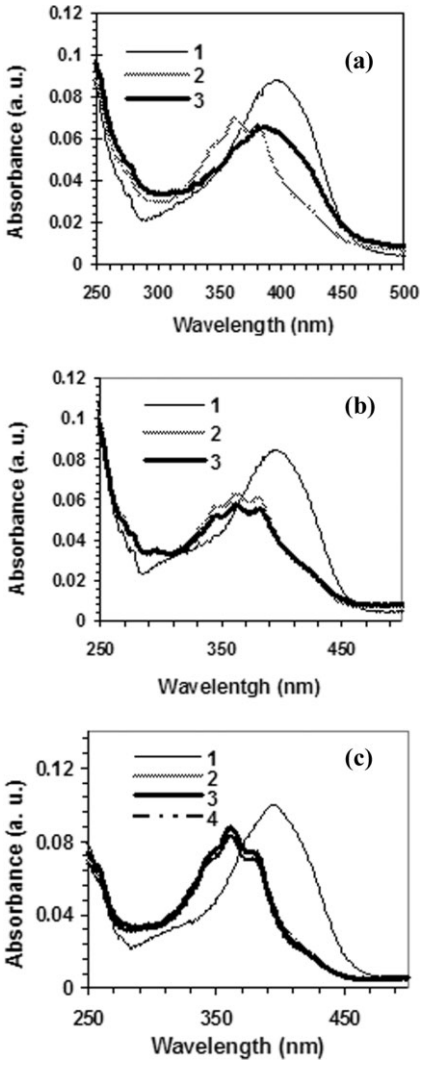

Figure 2. a) Return of the absorption spectrum of DMA-DPH to its original state (corresponding to the deprotonated form) after storage in air. UV spectra of 100 nm thick films of PMMA containing 2% w/w DMA-DPH and 4% w/w PAG: 1) unexposed, 2) exposed through a filter for 1500 s, 3) 48 h later (in air). b) Stabilization of the DMA-DPH absorption spectrum at a higher prebake temperature (130 °C). UV spectra 1 to 3 as for films in (a). c) Stabilization of the DMA-DPH absorption spectrum upon storage in a vacuum dessicator under reduced pressure (about 10 Torr; 1 Torr = 133.3 Pa). UV spectra 1–3 as for films in (a); Spectrum 4 was taken one week after exposure.

2.2. Acid-Induced Emission Changes of Red Emitters

To achieve red emission from the PVK layer, we dispersed a red emitter in the PVK matrix. Several red emitters, including the red probe 4-dimethylamino-4′-nitrostilbene (DANS) and the highly fluorescent dopant 4-(dicyanomethylene)-2-methyl-

6-[4-(dimethylaminostyryl)-4*H*-pyran], DCM,[20,21] well-known in OLED technology, were tested. In the case of DCM inserted into the PVK matrix, efficient energy transfer from the host polymer to the emitter (emission maximum at 605 nm) was observed. Exposure at 248 nm in the presence of PAG led to an acid-induced absorption shift and fluorescence quenching, as shown in Figure 3a and b, in which UV absorption and photoluminescence (PL) spectra of the DCM emitter inside the PMMA and PVK matrix, respectively, are presented. The proposed PAG-induced DCM protonation and bleaching is presented in Scheme 1. To verify that the bleaching of the DCM is indeed proton-induced, a solid acid was dispersed in the polymeric matrix along with the DCM emitter. The solid acid used was the well-known strong Brønsted acid $H_3PW_{12}O_{40}$ (dodecatungstophosporic acid). As can be seen in Figure 3c and d, in the presence of this acid, and as the concentration of the acid was increased by keeping the DCM concentration constant, the absorption and PL spectral changes of DCM were similar to the ones observed upon exposure (Fig. 3a and b).

Next, the DCM emitter was dispersed in the PVK matrix along with the green emitter DMA-DPH and the PAG. Our purpose was to examine the possibility of defining all three primary colors (RGB) in the same layer according to the patterning scheme presented in Scheme 2. In the unexposed areas, if efficient energy transfer from the host polymer and the green emitter to the red one is achieved, red emission is expected. After an optimum exposure dose, fluorescence quenching of the red emitter is expected, and green emission could be obtained if the green emitter DMA-DPH remains unprotonated to a significant extent. With subsequent irradiation, full protonation of the DMA-DPH emitter could be finally obtained, resulting in the blue emission of its photochemical product.

In the first experiments, when the DCM red emitter along with the DMA-DPH and the PAG were dispersed in the PVK host matrix, red emission was indeed obtained in the unexposed areas of the film. However, undesirable quenching of the total emission, and not the desired shift to lower wavelengths, was observed after exposure. It, thus, became evident that a better understanding of the parameters affecting the energy-transfer processes inside the PVK layer was needed in order to select an appropriate red emitter.

PVK is a large-bandgap conducting polymer, emitting in the violet-blue area of the optical spectrum. Its PL spectrum has been inserted in Figure 4a and b (curve 4 in both figures) to facilitate comparison. The absorption spectrum of the starting (unprotonated) form of DMA-DPH (Fig. 4a, curve 1) overlaps significantly with the PVK's emission, and, thus, efficient energy transfer from the host polymer to the green emitter is observed. In the case of the DCM starting form (Fig. 4a, curve 2), the degree of overlap with PVK emission is not as high but is still enough to achieve efficient energy transfer from PVK to the red emitter. Futhermore, DMA-DPH's emission inside the PVK matrix appears in the green wavelength region (the PL spectrum of DMA-DPH is also presented in Fig. 4a and b as curve 5 for comparison) and significantly overlaps with DCM's absorption as well. For the above reasons, in the case of the

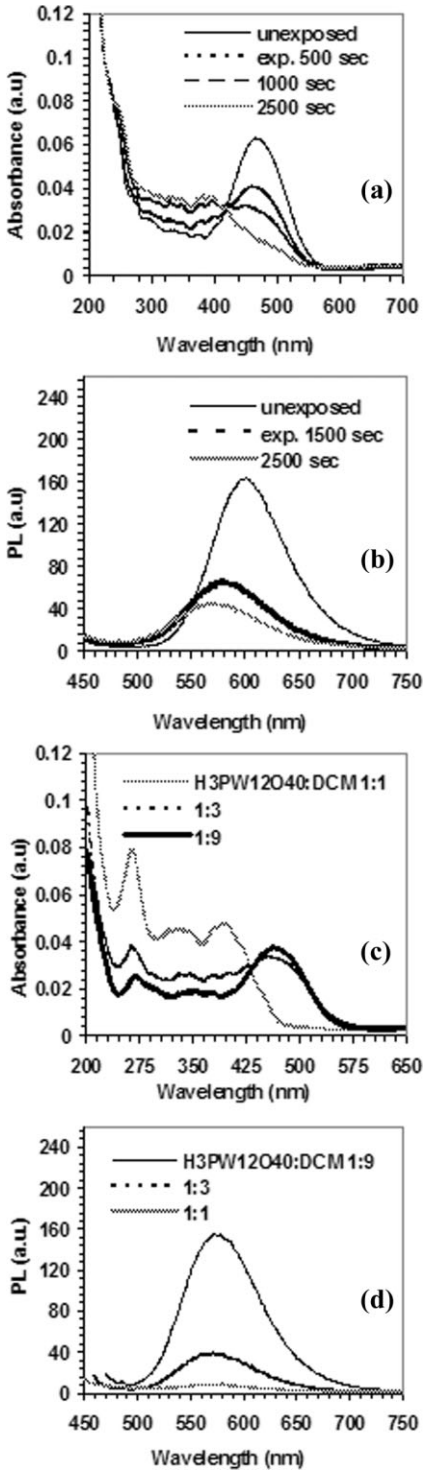

Figure 3. a) Photochemically induced changes in the absorption spectrum of 4 % w/w DCM dispersed in a PMMA matrix in the presence of 8 % w/w PAG (the spectra were taken after exposure through a 248 nm narrow band filter for 0, 500, 1000, and 2500 s). b) Photochemically induced changes in the PL spectrum of 4 % w/w DCM dispersed in a PVK matrix in the presence of 8 % w/w PAG (quenching of the probe's emission after exposure for 1500 and 2500 s). Changes in c) the UV absorption spectrum and d) the PL spectrum of DCM dispersed in either PMMA (c) or PVK (d) at a constant concentration of 1.5 % w/w of the polymer mass in the presence of $H_3PW_{12}O_{40}$ at molar ratios of 1:1, 1:3, and 1:9 relative to DCM.

ADVANCED FUNCTIONAL MATERIALS

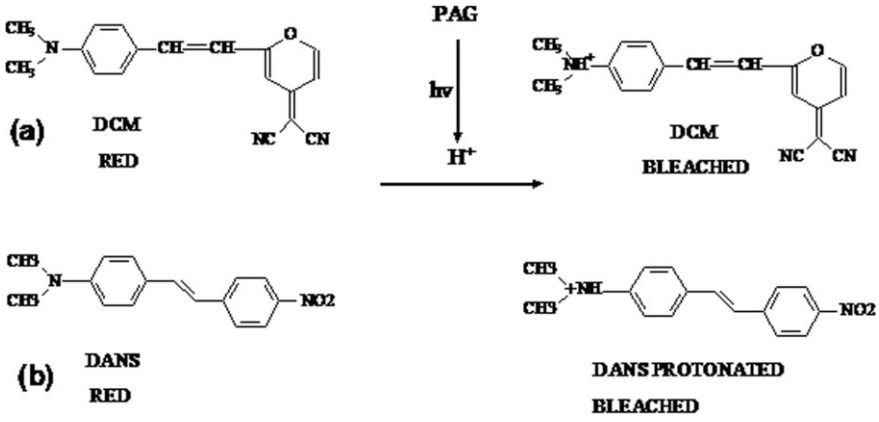

Scheme 1. Photogenerated acid-induced changes of the DCM and DANS emitters.

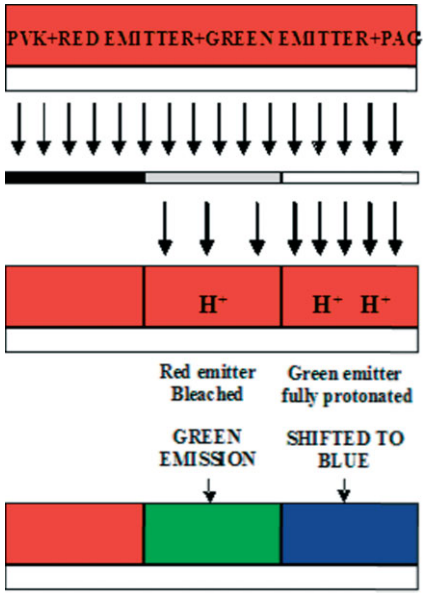

Scheme 2. Patterning scheme for the definition of RGB areas in a single PVK layer.

PVK film containing both emitters, the lower bandgap compound, that is, the red-emitting DCM, is expected to fluoresce. After exposure, DCM is protonated but its absorption spectrum (Fig. 4b, curve 2) overlaps significantly with the emission spectrum of PVK. However, this protonated form of DCM is not fluorescent. On the other hand, both forms of DMA-DPH absorb at lower wavelengths compared to the DCM protonated form. Thus, when DCM is protonated, energy transfer from PVK to the DCM protonated form takes place and the fluorescence of the whole system is quenched.

To achieve the desirable green and blue emission after exposure, we should use a red emitter whose absorption spectrum after exposure shifts significantly in order to absorb at lower wavelengths compared to DMA-DPH (both unprotonated and protonated forms). After several experiments, a well-known—especially in the field of polymerization processes monitoring—red probe, DANS,[22] was chosen (Scheme 1b). DANS initially absorbs strongly at about 440 nm (Fig. 4a, curve 3) but after exposure (or alternatively, after addition of solid acid in the film) a large absorption spectrum shift to the blue is observed (maximum at 340 nm, Fig. 4b, curve 3). The efficient energy transfer from PVK to the original DANS form and the quenching of its emission after exposure in the presence of PAG are shown in Figure 5a (see also Scheme 1b). When DANS along with DMA-DPH (in a molar ratio of 1:1) and the PAG were dispersed in a PVK matrix, the red fluorescence of DANS was observed in the unexposed film (Fig. 5b).

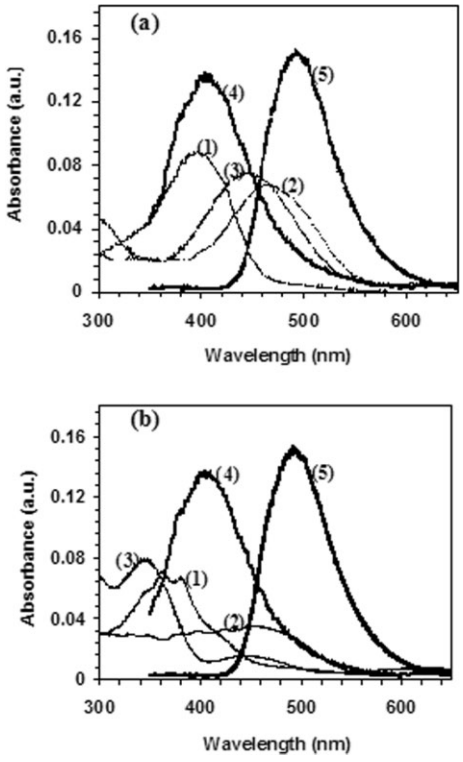

Figure 4. a,b) UV absorption spectra of the original molecules and the protonated molecules, respectively, of DMA-DPH, DCM, and DANS (curves 1, 2, and 3, respectively). All three emitters were inserted in the PMMA matrix at a concentration of 4 % w/w in the presence of PAG at a concentration of 8 % w/w. PL spectra corresponding to PVK (curve 4) and PVK with DMA-DPH added at a concentration of 2 % w/w (curve 5) are inserted as bold curves for comparison. The fluorescence intensity is given in arbitrary units.

After exposure, a 165 nm shift to shorter wavelengths (maximum at 440 nm), corresponding to the blue fluorescence of the DMA-DPH protonated molecule, was observed, as shown in Figure 5b. In this way RB emitting areas were photopatterned in a single layer of PVK. Color patterning of the PVK film, containing both emitters (at equal molar quantities) and the PAG (at double the molar ratio with respect to each emitter),

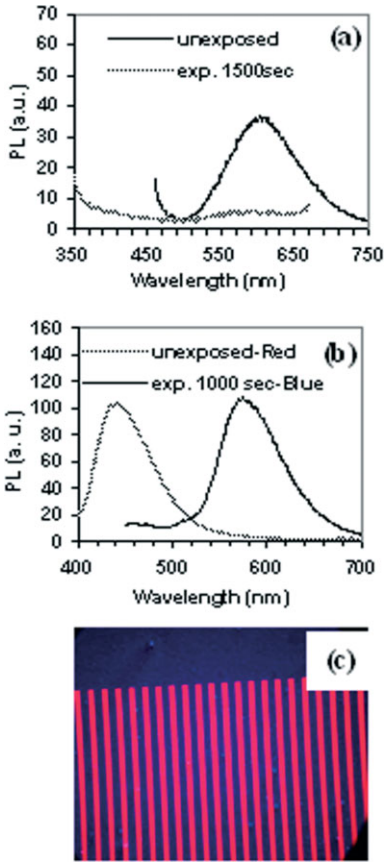

Figure 5. a) Energy transfer from PVK to the DANS emitter (2 % w/w) and fluorescence quenching after exposure (through a 248 nm filter) for 1500 s in the presence of the PAG (4 % w/w). b) PL spectra of a PVK film containing DANS, DMA-DPH (each probe at a concentration of 2 % w/w of polymer mass), and PAG (8 % w/w of polymer mass), before (red color pixel) and after exposure (blue color pixel) for 1000 s through a 248 nm filter. Excitation at 340 nm. c) The corresponding fluorescence pattern. The blue areas are the regions exposed through the photomask for 1000 s (film thickness: 100 nm). Line width: 15 μm.

results in red (unexposed) and blue (exposed) lines, as shown in Figure 5c.

2.3. RGB-Emitting Areas in a Single PVK Layer

In the experiment presented in Figure 5b and c, after exposure of the initial red-emitting film, only blue emission and not the intermediate green one was observed. This was attributed to the fact that protonation of both emitters takes place in parallel (as is expected by the similarity of their protonation sides, see Scheme 1) and both are practically fully protonated at the end of the exposure. For this reason, and after preliminary experiments, it was decided to insert DMA-DPH in a higher molar ratio (at least 2:1) relative to DANS (2 % and 1 % of the polymer mass, respectively) into the PVK matrix. In parallel, the amount of the PAG was decreased (to 4 % of the polymer mass) to facilitate the optimization of the processing conditions. It was believed that when DANS was protonated to a degree that would be adequate to bleach its fluorescence, the amount of DMA-DPH initial form (green-emitting) should still be enough to emit green light. At a larger exposure dose, DMA-DPH would be almost fully protonated and for this reason only blue emission was expected finally. In this way, the unexposed areas would remain red-emitting, the areas exposed with an intermediate dose would become green-emitting, and the fully exposed areas would emit in blue, according to Scheme 2. Indeed, using the material composition described above and the appropriate exposure dose, green-emitting areas were successfully defined. In Figure 6a and b we present RG- and RB-emitting areas, respectively, defined in the same photopatterned PVK film by using different exposure doses (see details in the caption of Fig. 6). The line dimensions shown are 25 μm. The use of a mask with gray (intermediate transparency) areas would allow the definition of all three (RGB) areas in one exposure step.

Light-emitting devices, with the structure: glass/indium tin oxide (ITO)/poly(3,4-ethylene dioxythiophene):poly(styrene sulfonate) (PEDOT:PSS) (40 nm)/emitting layer of PVK (containing DMA-DPH and DANS at a molar ratio of 2:1, and the dispersed PAG) (100nm)/Al (300 nm), were also demonstrated. Each pixel of these devices, corresponding to an unexposed area of PVK film, emits red light. Those pixels corresponding to areas exposed at an intermediate dose emit green and those corresponding to areas exposed at larger doses emit blue light. The normalized electroluminescence (EL) spectra and current density–voltage (J–V) plots of the three primary-color-emitting pixels successfully patterned in the same layer of PVK are presented in Figure 6c and d, respectively. The Commission Internationale de l'Éclairage (CIE) color coordinates (calculated in the specific case) of the blue-, green-, and red-emitting pixels are ($x = 0.17$, $y = 0.11$), ($x = 0.22$, $y = 0.61$), and ($x = 0.52$, $y = 0.36$), respectively. Further investigation of the material composition (emitters, relative ratios, and PAG ratio) and of the processing conditions (exposure dose) is needed in order to improve spectral purity and color quality.

The addition of the photoacid generator and the emitters into the polymer matrix does not significantly affect the electrical behavior of the diode, as one can see in Figure 6d. Only a small increase of the threshold voltage of the diodes that contain the additives (especially for the red-emitting pixels), compared to those based on pure PVK, is observed. On the other hand, a slight increase of current and decrease of threshold voltage was noticed in the exposed green and especially blue pixels relative to the red, unexposed ones. This observation probably indicates an increased current flow because of reduced charge trapping inside the exposed matrix. It should be mentioned that device optimization is in progress.

The color stability of the OLEDs during operation was also investigated in order to verify that the color of the pre-patterned emitting pixels remains stable during operation. As one can see in Figure 7a and b there was no change of the emitting color for the red and green pixels, respectively, as we continuously increased the DC bias from 18 to 30 V; similar spectra were recorded with increased EL intensities.

Finally, it should also be mentioned that by varying the amount of PAG and keeping both emitter concentrations con-

ADVANCED FUNCTIONAL MATERIALS

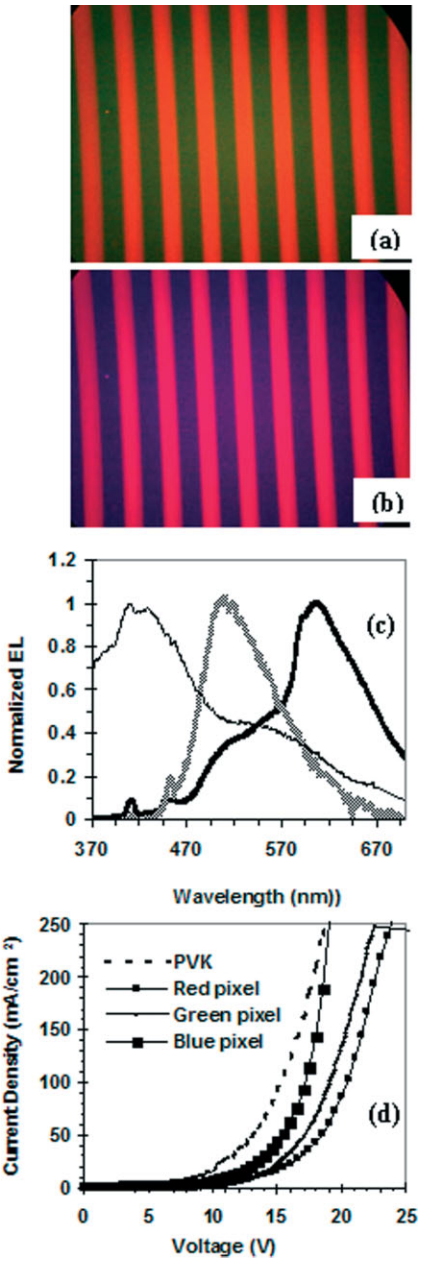

Figure 6. a, b) Fluorescence patterns on a single PVK layer (containing 2 % (w/w) DMA-DPH, 1 % (w/w) DANS, and 4 % (w/w) PAG): red lines (unexposed)–green lines (exposed for 1000 s)–blue lines (exposed for 2000 s). Film thickness: 100 nm. Lines width: 25 μm. c) Normalized electroluminescence (EL) spectra and d) current density–voltage (*J*–*V*) plots of OLEDs having the structure glass/indium tin oxide (ITO)/poly(3,4-ethylene dioxythiophene):poly(styrene sulfonate) (PEDOT:PSS) (40 nm)/active layer (100nm)/Al (300 nm). The active layer was PVK containing 2 % w/w DMA-DPH, 1 % w/w DANS, and 4 % w/w PAG, either unexposed (red pixel) or exposed through a filter for 1000 s (green pixel) and 2000 s (blue pixel).

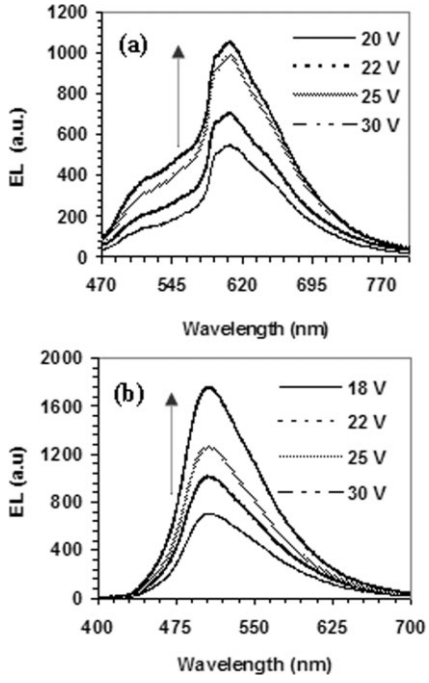

Figure 7. Color stability of the EL spectra of a) red-emitting (unexposed) and b) green-emitting (exposed through the filter for 1000 s) OLEDs, both having the same structure as in Figure 6, for increased DC bias from 18 to 30 V. Each value of the DC voltage was applied for 30 min.

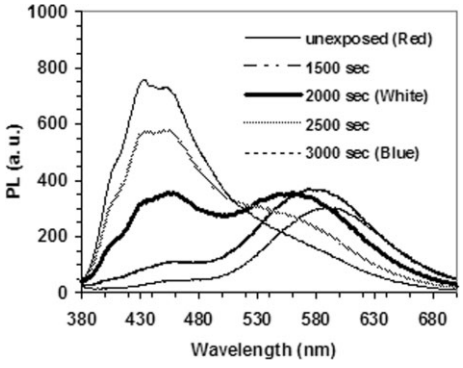

Figure 8. PL spectra of a PVK film containing DANS (1 % w/w), DMA-DPH (2 % w/w), and the PAG (3 % w/w), before (red color) and after exposure for 1500 s (yellow color), 2000 s (white color), and 3000 s (blue color).

stant, it was found that for smaller PAG amounts, and with careful control of the exposure dose, we were able to tune the emitting color in the whole range from red to blue, even achieving white-light emission. A representative case can be seen in Figure 8, where the PL spectra of DANS (1 %), DMA-DPH (2 %), and PAG (3 % w/w) inserted in a single PVK layer exposed through a filter for various doses are presented.

3. Conclusions

Areas emitting all three primary colors, red, green, and blue, were defined in a single layer of the wide-bandgap conducting polymer, poly(9-vinylcarbazole), using a suitable green emitter DMA-DPH along with the red emitter DANS. The selected emitters were dispersed in the PVK films in the presence of a photoacid generator, and their emission was tuned through

photochemically induced transformations. In particular, the photogenerated acid induces bleaching of the red emitter and emission shift of the green one, allowing definition of the three primary color emitting areas. Electroluminescence data and stability studies (lifetime and color stability) indicate that the proposed approach is viable for potential application in OLED technology, while further material and process improvements are in progress.

4. Experimental

Materials and Instrumentation: Fluorescent dyes 1-(4′-dimethyl-aminophenyl)-6-phenyl-1,3,5-hexatriene (DMA-DPH), and 4-dimethylamino-4′-nitrostilbene (DANS) were purchased from Fluka. The photoacid generators (PAGs) used were triphenylsulfonium hexafluoroantimonate and triphenylsulfonium trifluoromethane sulfonate purchased from Midori Kagaku. Poly(9-vinylcarbazole) (PVK) was purchased from Aldrich and used with no further purification, while the PMMA polymer was Elvacite 2041 purchased from DuPont. Poly(3,4-ethylene dioxythiophene):poly(styrene sulfonate) (PEDOT:PSS) was purchased from Aldrich. For absorption spectra a Perkin–Elmer Lambda-40 spectrometer was employed. Fluorescence and excitation measurements were recorded with a Perkin–Elmer LS-50B fluorescence spectrometer. Fluorescence images were taken using the Axioscope 2 plus epifluorescence microscope equipped with a Sony Cyber-Shot digital camera.

Polymeric Film Preparation and Processing: Solutions containing PVK (40 mg mL^{-1} in 1,1,2,2-tetrachloroethane) and PMMA (4 % w/w in methylisobutylketone, MIBK) were prepared. In some solutions, the PAG (4 %, 6 %, and 8 % of polymer mass) and the fluorescence emitter DMA-DPH (1 %, 2 %, and 4 % of polymer mass) were added in various concentrations. Some other solutions were made by adding the PAG along with the DMA-DPH and the DANS emitter at various concentrations (from 1:10 to 10:1 of the DMA-DPH amount). Films were spin-coated from filtered solutions at 2000 rpm and then baked on a hotplate at 80 °C for 10 min. Film thicknesses were measured with an Ambios profilometer. Photoacid generation was induced by exposing films to a 500 W Oriel Hg–Xe exposure lamp through a 248 nm narrowband filter (6.5 nm half-band width) for various times. The incident power was measured with an IL 1700 International Light radiometer and was found to be (0.21 ± 0.02) mJ s^{-1}.

Electroluminescent Device Fabrication and Characterization: For the electroluminescent devices, 100 nm thick films of PVK were spun on ITO glass substrates (product of Aldrich) at 2000 rpm and baked at 80 °C for 10 min. ITO-coated glass was precleaned in an ultrasonic bath with a sequence of acetone, isopropyl alcohol, and deionized (DI) water and treated with an oxygen plasma to improve the ITO properties. Prior to the PVK layer, a 40 nm thick film of PEDOT:PSS was spin-coated (at 4000 rpm and baked at 125 °C for 15 min) in order to improve hole injection and substrate smoothness and enhance the performance of the electroluminescent device. 300 nm thick aluminum cathode electrodes were deposited on top of the PVK films by vacuum evaporation. All the testing devices had an active area of 2 mm × 2 mm. Current density–voltage (J–V) measurements were obtained using a programmable Keithley 230 voltage source and a 195 A multimeter. EL spectra were recorded with a USB 2000-UV-vis miniature fiber-optic spectrometer.

Received: February 26, 2007
Revised: June 4, 2007
Published online: October 31, 2007

[1] a) J. H. Burroughes, D. D. C. Bradley, A. R. Brown, R. N. Marks, K. Mackay, R. H. Friend, P. L. Burns, A. B. Holmes, *Nature* **1990**, *347*, 539. b) R. H. Friend, R. W. Gymer, A. B. Holmes, J. H. Burroughes, R. N. Marks, C. Taliani, D. D. C. Bradley, D. A. Dos Santos, J. L. Brédas, M. Lögdlund, W. R. Salaneck, *Nature* **1999**, *397*, 121.

[2] a) C. W. Tang, S. A. VanSlyke, *Appl. Phys. Lett.* **1987**, *51*, 913-5. b) G. Gustafsson, Y. Cao, G. M. Treacy, F. Klavetter, N. Colaneri, A. J. Heeger, *Nature* **1992**, *357*, 477.

[3] a) D. A. Pardo, G. E. Jabbour, N. Peyghambarian, *Adv. Mater.* **2000**, *12*, 1249. b) B. W. D'Andrade, J. Brooks, V. Adomovich, M. E. Thomson, S. R. Forrest, *Adv. Mater.* **2002**, *14*, 1032. c) M. Pfeiffer, S. R. Forrest, K. Leo, M. E. Thomson, *Adv. Mater.* **2002**, *14*, 1633. d) J. S. Kim, R. H. Friend, I. Grizzi, J. H. Burroughes, *Appl. Phys. Lett.* **2005**, *87*, 23 506. e) X. H. Yang, D. C. Muller, D. Neher, K. Meerholz, *Adv. Mater.* **2006**, *18*, 948. f) B. Liang, C. Y. Jiang, Z. Chen, X. J. Zhang, H. H. Shi, Y. Chao, *J. Mater. Chem.* **2006**, *16*, 1281.

[4] a) G. Gu, V. Bulovic, P. E. Burrows, S. R. Forrest, M. E. Thompson, *Appl. Phys. Lett.* **1996**, *68*, 2606. b) G. Parthasarathy, G. Gu, S. R. Forrest, *Adv. Mater.* **1999**, *11*, 907. c) X. Jiang, Z. Zhang, W. Zhao, W. Zhu, B. Zhang, S. Xu, *J. Phys. D: Appl. Phys.* **2000**, *33*, 473. d) B. W. D'Andrade, M. E. Thompson, S. R. Forrest, *Adv. Mater.* **2002**, *14*, 147.

[5] a) T. R. Hebner, C. C. Wu, D. Marcy, M. H. Lu, J. C. Sturm, *Appl. Phys. Lett.* **1998**, *72*, 519. b) J. H. Choi, K. H. Kim, S. J. Choi, H. H. Lee, *Nanotechnology* **2006**, *17*, 2246.

[6] a) J. Kido, K. Hongawa, K. Okuyama, K. Nagai, *Appl. Phys. Lett.* **1994**, *64*, 815. b) J. Kido, M. Kimura, K. Nagai, *Science* **1995**, *267*, 1332. c) C.-H. Kim, J. Shinar, *Appl. Phys. Lett.* **2002**, *80*, 2201. d) Y.-S. Huang, J.-H. Jou, W.-K. Weng, J.-M. Liu, *Appl. Phys. Lett.* **2002**, *80*, 2782.

[7] a) Y. Yang, Q. Pei, *J. Appl. Phys.* **1997**, *81*, 3294. b) Y.-Z. Lee, X. Chen, M.-C. Chen, S.-A. Chen, *Appl. Phys. Lett.* **2001**, *79*, 308. c) G. Tu, Q. Zhou, Y. Cheng, L. Wang, D. Ma, X. Jing, F. Wang, *Appl. Phys. Lett.* **2004**, *85*, 2172.d) J. Y. Li, D. Liu, C. Ma, O. Lengyel, C.-S. Lee, C.-H. Tung, S. Lee, *Adv. Mater.* **2004**, *16*, 1538. e) C.-Y. Chuang, P.-I. Shih, C.-H. Chien, F.-I. Wu, C.-F. Shu, *Macromolecules* **2007**, *40*, 247.

[8] a) M. Granstrom, O. Inganäs, *Appl. Phys. Lett.* **1996**, *68*, 147. b) S. Tasch, E. J. W. List, O. Ekström, W. Graupner, G. Leising, P. Schlichting, U. Rohr, Y. Geerts, U. Scherf, K. Müllen, *Appl. Phys. Lett.* **1997**, *71*, 2883.

[9] a) J. Kido, H. Shionoya, K. Nagai, *Appl. Phys. Lett.* **1995**, *67*, 2281. b) B. W. D'Andrade, R. J. Holmes, S. R. Forrest, *Adv. Mater.* **2004**, *16*, 624. c) S. Tokito, T. Iijima, T. Tsuzuki, F. Sato, *Appl. Phys. Lett.* **2003**, *83*, 2459. d) E. L. Williams, K. Haavisto, J. Li, G. E. Jabbour, *Adv. Mater.* **2007**, *19*, 197.

[10] a) Y. Sun, N. C. Giebink, H. Kanno, B. Ma, M. E. Thompson, S. R. Forrest, *Nature* **2006**, *440*, 908. b) G. Schwartz, K. Fehse, M. Pfeiffer, K. Walzer, L. Leo, *Appl. Phys. Lett.* **2006**, *89*, 083 509.

[11] a) M. Mazzeo, D. Pisignano, F. D. Sala, J. Thompson, R. I. R. Blyth, G. Gigli, R. Cingolani, *Appl. Phys. Lett.* **2003**, *82*, 334. b) S. P. Singh, Y. N. Mohapatra, M. Qureshi, S. S. Manoharan, *Appl. Phys. Lett.* **2005**, *86*, 113 505. c) Q. J. Sun, B. H. Fun, Z. A. Tan, C. H. Yang, Y. F. Li, *Appl. Phys. Lett.* **2006**, *88*, 163 510.

[12] a) S. Shirai, J. Kido, *J. Photopolym. Sci. Technol.* **2001**, *14*, 317. b) G. Trattnig, A. Pogantsch, G. Langer, W. Kern, E. Zojer, *Appl. Phys. Lett.* **2002**, *81*, 4269. c) A. Pogantsch, S. Rentenberger, G. Langer, J. Keplinger, W. Kern, E. Zojer, *Adv. Funct. Mater.* **2005**, *15*, 403. d) X. Y. Deng, K. Y. Wong, Y. Q. Mo, *Appl. Phys. Lett.* **2007**, *90*, 063 505.

[13] a) C. D. Müller, A. Falcou, N. Reckefuss, M. Rojhan, V. Wiederhirn, P. Rudati, H. Frohne, O. Nuyken, H. Becker, K. Meerholz, *Nature* **2003**, *421*, 829. b) M. C. Gather, A. Köhnen, A. Falcou, H. Becker, K. Meerholz, *Adv. Funct. Mater.* **2007**, *17*, 191.

[14] a) J. M. Kim, T. E. Chang, J. H. Kang, K. H. Park, D. K. Hang, K. D. Ahn, *Angew. Chem. Int. Ed.* **2000**, *39*, 1780. b) J. M. Kim, T. E. Chang, J. H. Kang, D. K. Hang, K. D. Ahn, *Adv. Mater.* **1999**, *11*, 1499. c) J. M. Kim, J. H. Kang, D. K. Han, C. W. Lee, K. D. Ahn, *Chem. Mater.* **1998**, *10*, 2332. d) A. M. Vekselman, C. Zhang, *Chem. Mater.* **1997**, *9*, 1942.

ADVANCED FUNCTIONAL MATERIALS

[15] a) B. Lu, J. W. Taylor, F. Cerrina, C. P. Soo, A. J. Boordillion, *J. Vac. Sci. Technol. B* **1999**, *17*, 33 450. b) P. L. Zhang, S. Webber, J. Mendelhall, J. Byers, K. Chao, *Proc. SPIE* **1998**, *3333*, 794. c) U. Okoroanyanwu, J. D. Byers, T. Cao, S. E. Webber, C. G. Wilson, *Proc. SPIE* **1998**, *3333*, 747.

[16] a) G. Pistolis, S. Boyatzis, M. Chatzichristidi, P. Argitis, *Chem. Mater.* **2002**, *14*, 790. b) G. Pistolis, A. Malliaris, *Langmuir* **1997**, *13*, 1457. c) G. Pistolis, A. Malliaris, *Chem. Phys.* **1998**, *226*, 83.

[17] a) J. Kido, K. Hongawa, K. Okuyama, K. Nagai *Appl. Phys. Lett*. **1993**, *63*, 2627. b) T. Dantas de Morais, F. Chaput, K. Lahlil, J.-P. Boilot. *Adv. Mater.* **1999**, *11*, 107. c) C.-L. Lee, R. Ragini Das, J.-J. Kim, *Chem. Mater*. **2004**, *16*, 4642. d) Y. H. Niu, B. Q. Chen, T. D. Kim, M. S. Liu, A. K. Y. Jen, *Appl. Phys. Lett.* **2004**, *85*, 5433. e) F. C. Chen, Y. Yang, M. E. Thompson, J. Kido *Appl. Phys. Lett.* **2002**, *80*, 2308.

[18] H. Ito, G. Breyta, D. C. Hofer, R. Sooriyakumaran, K. Petrillio, D. Seeger, *J. Photopolym. Sci. Technol.* **1994**, *7*, 433.

[19] S. A. MacDonald, C. G. Willson, J. M. J. Frechet, *Acc. Chem. Res.* **1994**, *27*, 151.

[20] C. W. Tang, S. A. Van Slyke, C. H. Chen, *J. Appl. Phys.* **1989**, *65*, 3610.

[21] a) J. Kido, K. Hongawa, K. Okugama, N. Nagai, *Appl. Phys. Lett*. **1994**, *64*, 815. b) H. Suzuki, S. Hoshino, *J. Appl. Phys.* **1996**, *79*, 8816. c) V. Bulovic, A. Shoustikov, M. A. Baldo, E. Bose, V. G. Gozlov, M. E. Thomson, S. R. Forrest, *Chem. Phys. Lett.* **1998**, *287*, 455. d) B.-J. Jung, C.-B. Yoon, H.-K. Shim, L.-M. Do, T. Zyung, *Adv. Funct. Mater*. **2001**, *11*, 430. e) T.-H. Liu, C.-W. Iou, C. H. Chen, *Appl. Phys. Lett*. **2003**, *83*, 5241. f) C.-L. Chiang, M.-F. Wu, D.-C. Dai, W.-S. Wen, J.-K. Wang, C.-T. Chen, *Adv. Funct. Mater*. **2005**, *15*, 231.

[22] a) E. Lippert, W. Lüder, F. Moll, W. Nägelle, H. Boos, H. Prigge, *Angew. Chem*. **1961**, *73*, 695. b) A. P. de Silva, H. Q. Nimal Gunaratne, T. Gunnlougsson, A. J. M. Huxley, C. P. McCoy, J. T. Rademacher, T. E. Rice, *Chem. Rev.* **1997**, *97*, 1515. c) J. F. Jager, A. M. Sarker, D. C. Neckers, *Macromolecules* **1999**, *32*, 8791. d) A. M. Moran, G. P. Bartholomew, G. C. Bazan, A. M. Kelley, *J. Phys. Chem. A* **2002**, *106*, 4928. e) T. Nakabayashi, Md. Wahadoszamen, N. Ohta, *J. Am. Chem. Soc*. **2005**, *127*, 7041.